1 3D Numerical and Experimental Cases

1.1 Cylindrical Mesh:

Initially, to asses the effectiveness of the proposed method, a cylindrical mesh (regular geometry) and a breast mesh (irregular geometry) with background optical properties as $\mu_a = 0.01$ mm^{-1}, $\mu_s' = 1$ mm^{-1} and uniform refractive index of 1.33 is considered. The diameter of cylindrical mesh is 86 mm and height was 110 mm centered around origin. It had two cylindrical targets mimicking tumors located diagonally opposite to each other ((-15,15,0) and (15,-15,0)) with a radius of 7.5 mm and optical properties being $\mu_a = 0.02$ mm^{-1}, $\mu_s' = 1$ mm^{-1}. The two-dimensional cross sections of the target 3D volume is displayed in increments of 10 mm spanning from z =-55 mm to z=55 mm from left-hand side to right-hand side, are shown in top row of Fig. 1. To generate numerical experimental data, a fine mesh having 101106 nodes (corresponding to 503023 linear tetrahedral elements) is used. This data was added with 1% normally distributed gaussian noise to result in experimental mimicking data. The reconstructions were carried on a FEM mesh consisting of 31446 nodes (corresponding to 152925 linear tetrahedra elements). The data-collection system had 16 fibers arranged in a circular fashion at z=0 mm, where when one fiber acts as a source, rest act as detectors. This set up results 240 number of measurements (m). Each source was modeled as Gaussian source having full width at half maximum of 3 mm to mimic the experimental case[1] and is placed at one mean transport length inside the boundary.

1.2 Breast Mesh:

In case of breast mesh, the background optical properties were chosen same as earlier case, here only one spherical target is placed at the centre of imaging domain with a radius of 7.5 mm and optical properties similar to earlier case. The target distribution is shown in Fig. 2 as the first column. The numerical experimental data was generated on the finite element mesh having 96088 nodes (corresponding to 595162 linear tetrahedral elements), like earlier case 1% noise was added to this data. A coarser mesh having 28640 nodes (corresponding to 132110 linear tetrahedral elements) was used in the reconstruction. In the both case, noisy data was calibrated using the coarser mesh to remove any source/detector biases and modeling errors.

1.3 Gelatin Phantom Experiment:

To effectively evaluate the proposed method in comparison to standard method, the experimental data collected around the boundary of a gelatin phantom was used with standard and proposed method case. This gelatin phantom was cylindrical in shape and had a diameter of 86 mm, height 60 mm was fabricated following the procedure as explained in [2] and mixtures of 80% of deionised water and 20% of gelatin (G2625, Sigma Inc) along with India ink for absorption and Titanium oxide(TiO_2) for scattering was used to build the background with the optical properties $\mu_a = 0.008$ mm^{-1}, $\mu_s' = 0.9$ mm^{-1} at 785 nm wavelength. To mimic the tumor characteristics, along the Z direction a cylindrical hole of dimension radius of 8 mm and height of 59 mm was made and filled with intra-lipid mixed with India ink to act as an absorptive target having the optical properties $\mu_a = 0.02$ mm^{-1},

$\mu_s' = 1.0$ mm^{-1}. A cylindrical mesh consisting 36425 nodes corresponding to 177662 linear tetrahedral elements was used and the experimental data were also calibrated using a reference homogenous phantom data. The 2D distributions of expected 3D volume in steps of 5.45 mm spanning from z = -30 mm to z = 30 mm (left to right) is given in the top row of Fig. 3. The data-collection geometry was similar to numerical case and the was collected at wavelength of 785 nm.

2 Results

The reconstruction results corresponding numerical evaluation of the method are given in Fig. 1 and 2 corresponding to cylindrical mesh and breast mesh cases. The results indicate that the contrast recovery in these 3D cases is much poorer and results from proposed method looks more smoothened compared to standard reconstruction (Eq. 4) in the multiple targets case (cylindrical mesh, Fig. 1). The experimental results obtained using gelatin phantom data are given in Fig. 3 along with one-dimensional cross-sectional profiles on the right hand side of the same figure. The proposed method contrast recovery was higher than the standard method in this case and resulted qualitatively similar reconstruction distributions visually. For the standard case, $\lambda = 0.1$, 1, and 0.5 for cylindrical, breast, and phantom cases was used, which gave the best estimates of optical properties.

The total computation time along with number of iterations taken for convergence to the solution was recorded and same is reported in Table-1 for the results presented in Figs. 1,

2, and 3. The computation results indicate that the proposed algorithm results in computationally efficient scheme compared to others.

List of Tables

List of Figures

Tables

Update Equation	**Cylindrical Mesh** (Fig. 1)	**Breast Mesh** (Fig. 2)	**Phantom Mesh** (Fig. 3)
Eq. 4 (Standard)	23,214(16)	16,314(15)	28,168(20)
Eq. 5 (Standard)	4,058(16)	3,005(15)	5,116(20)
Eq. 7 (Proposed)	1,769(7)	1,012(5)	1,781(7)

Table 1: Comparison of total computational time (in seconds) for the three cases considered in this work. The last row gives the proposed method timing results. First two rows corresponding to Eqs. 4 and 5 gives the timing for standard methods. The total number of iterations taken to converge are given in the parenthesis.

Figures

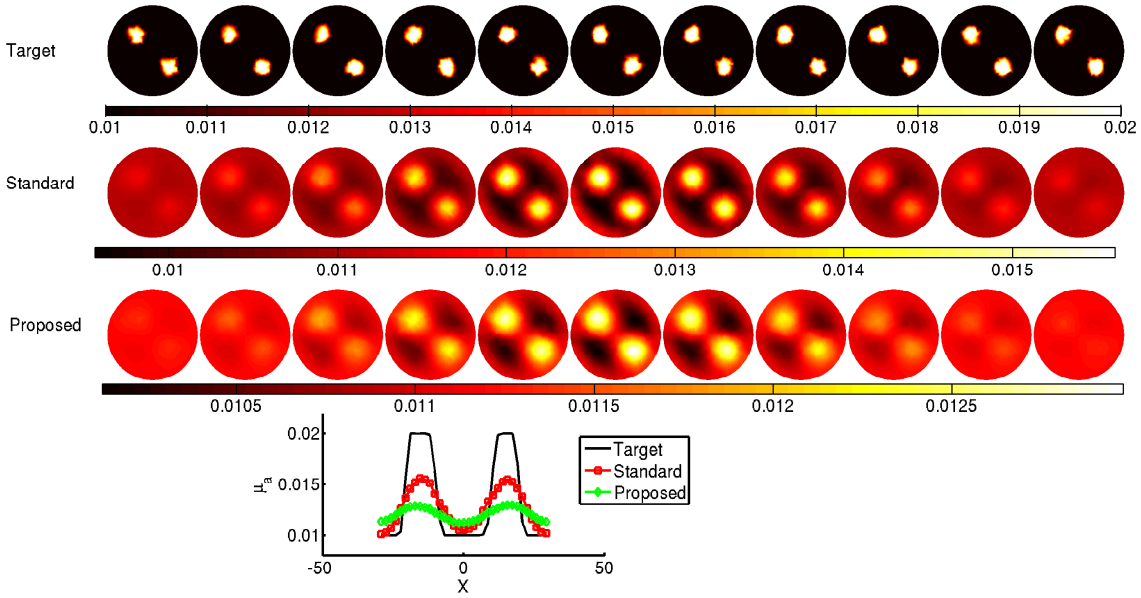

Figure 1: Comparison of reconstruction performance in 3D cylindrical mesh using the standard and proposed optimization work. Here two cylindrical anomalies are separated along the diagonal whose target is shown on top. The reconstruction of the image using 1% noisy data is shown for both proposed and standard technique. Corresponding line profile is shown through the plot x=-y line the center (z=0).

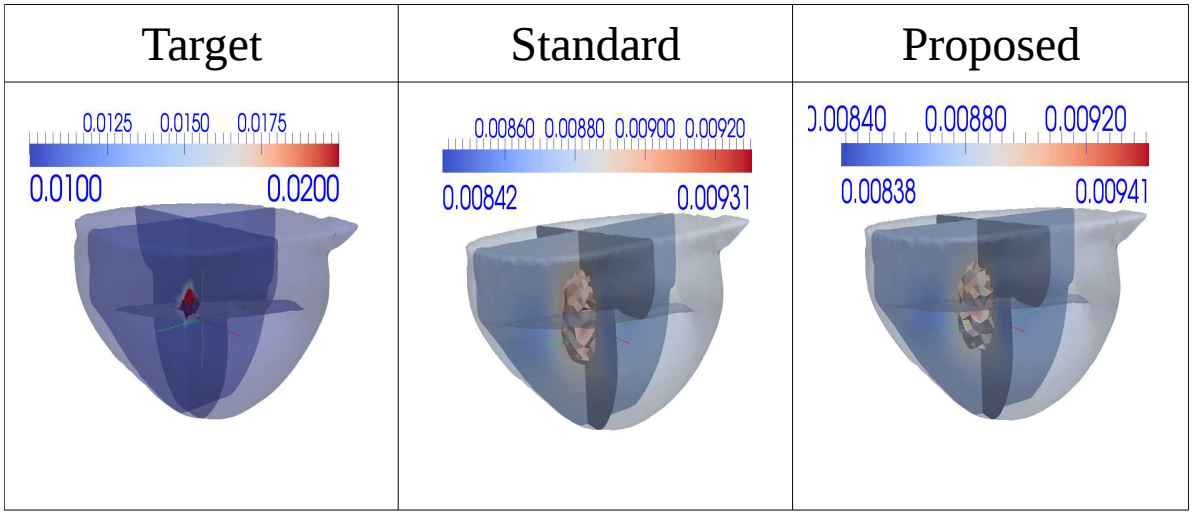

Figure 2: Comparison of reconstruction performance in breast mesh using the standard and proposed optimization work. Here we have a single anomaly whose target along with reconstruction of the image using 1% noisy data is shown for both proposed and standard technique.

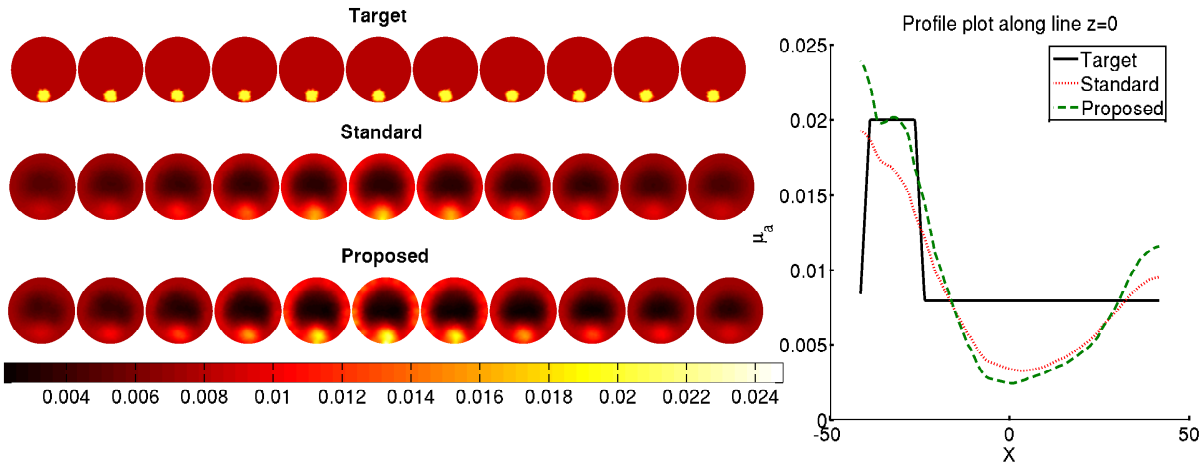

Figure 3: Comparison of reconstructions using the standard technique and optimized case for the experimental data case. We have shown the target μ_a and reconstruction with proposed and standard techniques. Also shown is the profile plot across the line z=0 in this case.

References

[1] T. O. Mcbride, B. W. Pogue, S. Jiang, U. L. Osterberg, and K. D. Paulsen, "A parallel-detection frequency-domain near-infrared tomography system for hemoglobin imaging of the breast in vivo," Rev. Sci. Instr. **72**, 1817–1824 (2001).

[2] B. W. Pogue and M. Patterson, "Review of Tissue Simulating Phantoms for Optical Spectroscopy, Imaging and Dosimetry", J. Biomed. Opt, **11**, 041102, (2006).